

Visible-Light Driven Ag-TiO₂ Photocatalyst Prepared by Simple Physical Mixing of Commercial Colloidal Silver and TiO₂ Suspensions for Indoor VOC Degradation

Woosung Choi¹ and Wang Kai Y²

¹University High School, 4771 Campus Drive, Irvine, California, 92612, United States;

²Northwood High School, 4515 Portola Pkwy, Irvine, California, 92620, United States

ABSTRACT

Sick Building Syndrome arises from volatile organic compounds (VOCs) emitted indoors by household materials. Photocatalytic oxidation with TiO₂ has been studied to reduce indoor VOCs, but TiO₂ mainly absorbs ultraviolet light. Indoor lighting is dominated by visible light, so the use of TiO₂ indoors becomes limited. In previous studies, AgNP was added on TiO₂ to push its activation range into visible light, mostly by sol-gel methods. This research examined whether simply mixing two commercial products, a colloidal silver solution and a TiO₂, can produce a visible-light driven AgNP-TiO₂ without chemical synthesis. The key question was whether visible-light activation through SPR sensitization requires direct Ag-O-Ti chemical bonding, or whether physical proximity between AgNP and TiO₂ in the dried coating is sufficient. 1 wt% and 5 wt% AgNP-TiO₂ were prepared by physical mixing and characterized by UV-Vis spectrophotometry and X-ray diffraction (XRD). SPR peak was observed at around 430 nm. XRD confirmed the anatase phase of TiO₂ with rutile, and no peak shift was observed after AgNP addition. The samples were sprayed on paint-coated containers, and VOC removal was measured under UV and fluorescent lamps. VOC removal under fluorescent light followed the order of 5 wt% > 1 wt% > pure TiO₂. The visible-light activity in the absence of a chemical synthesis step can be understood from the photon-based nature of the SPR effect. AgNP absorbs visible photons by plasmonic oscillation of surface electrons, and the energy is transferred to TiO₂ via near-field coupling. Such a process does not require Ag-O-Ti bonding.

Keywords: Titanium Dioxide; Silver Nanoparticles; Visible-Light Photocatalysis; Surface Plasmon Resonance; Physical Mixing; Volatile Organic Compounds; Sick Building Syndrome

INTRODUCTION

In modern society, people are spending an increasing amount of their time inside buildings, and the quality of indoor air has become an important factor for human health (1). One of the indoor air problems that draws attention in recent years is Sick Building Syndrome (SBS), a condition that affects residents and workers of certain buildings with headaches, respiratory irritation, fatigue, and allergic reactions (2, 3). According to the

Corresponding author: Woosung Choi, E-mail: woosungchoi38@gmail.com.

Copyright: © 2026 Woosung Choi et al. This is an open access article distributed under the terms of the Creative Commons Attribution License, which permits unrestricted use, distribution, and reproduction in any medium, provided the original author and source are credited.

Accepted June 4, 2026

<https://doi.org/10.70251/HYJR2348.43441450>

1984 World Health Organization (WHO) report, up to 30% of newly constructed or remodeled buildings worldwide may receive complaints related to indoor air quality (4). People spend more than 90% of their time indoors, and the inhalation of indoor air therefore becomes the largest pathway through which airborne pollutants enter the human body (5).

The main cause of SBS is the emission of volatile organic compounds (VOCs) from indoor materials such as paints, adhesives, carpets, and cleaning supplies. Representative VOCs found indoors include formaldehyde, benzene, xylene, and styrene, all of which are known to cause health problems ranging from mild dizziness to carcinogenic effects (6). Among these sources, paint applied on indoor walls is one of the materials that release VOCs continuously over an extended period, which makes paint a representative source for examining VOC removal performance in laboratory conditions.

Several approaches have been suggested to reduce indoor VOC levels. Continuous mechanical ventilation can dilute VOC concentrations, but it is not always practical because of energy cost and the limited possibility of installation in existing buildings. Thermal oxidation can decompose VOCs into harmless substances such as water and carbon dioxide, however, the operation temperature usually exceeds 315 °C, which makes the method unsuitable for indoor application (7). As an alternative, photocatalytic oxidation has been studied as a method that operates at room temperature with light energy (8). In photocatalytic oxidation, a photocatalyst absorbs light, generates electron-hole pairs, and produces reactive oxygen species that decompose VOCs into water and carbon dioxide (9).

Among various photocatalysts, titanium dioxide (TiO₂) has been widely used for VOC degradation because it is chemically stable, non-toxic, and inexpensive (10). TiO₂ exists in three crystalline phases, anatase, rutile, and brookite, and the anatase phase generally shows higher photocatalytic activity than the others. However, the band gap of anatase TiO₂ is about 3.2 eV, which corresponds to the ultraviolet (UV) region of light. This means that TiO₂ mainly absorbs UV light and shows limited activity under visible light. UV light occupies only a small fraction of indoor lighting, so the practical use of TiO₂ for indoor VOC removal becomes limited (11).

To extend the activation range of TiO₂ into the visible region, two main strategies have been studied. One is dye sensitization, where organic dye molecules adsorbed on the TiO₂ surface absorb visible light and inject electrons

into the conduction band of TiO₂ (12). Although this method works, organic dyes are expensive and most dyes carry intrinsic colors that interfere with the appearance of treated surfaces. The other strategy uses plasmonic metal nanoparticles such as silver (Ag) or gold (Au) (13). When metal nanoparticles of a certain size range are illuminated by visible light, the conduction electrons on the particle surface undergo collective oscillation, a phenomenon known as surface plasmon resonance (SPR). The SPR effect enables the nanoparticle to absorb visible photons efficiently, and the absorbed energy can be transferred to a nearby semiconductor such as TiO₂ through near-field electromagnetic coupling or by hot electron injection. AgNP is more cost-effective than AuNP and is widely accessible through commercial colloidal silver solutions sold for antimicrobial purposes, which makes it a suitable candidate for indoor applications.

Most of the previous studies on AgNP-TiO₂ photocatalysts have used wet chemical synthesis, sol-gel methods, or photodeposition to attach AgNP onto the TiO₂ surface. These methods generally produce direct chemical contact between AgNP and TiO₂, including the possible formation of Ag-O-Ti bonding at the interface. While such methods provide controlled deposition, they require laboratory equipment and trained handling, which is a barrier for practical application at the household scale.

In this research, a different approach was examined, in which a commercial TiO₂ spray and a commercial colloidal silver solution were simply physically mixed and the obtained mixture was tested as a visible-light photocatalyst for indoor VOC removal. This study has two objectives. The first objective is to test whether a simple physical mixing of two pre-existing commercial products can produce a visible-light driven photocatalyst without any chemical synthesis procedure, which would provide an accessible alternative to the conventional synthesis methods mentioned above. The second objective is to address a mechanistic question in plasmonic photocatalysis, namely whether the SPR-mediated energy transfer from AgNP to TiO₂ requires direct Ag-O-Ti chemical bonding at the interface, or whether physical proximity between AgNP and TiO₂ in the dried coating is sufficient. Since the physical mixing approach does not form chemical bonding between AgNP and TiO₂, as confirmed later by the XRD analysis, it provides a suitable system to test this question directly. To investigate these objectives, AgNP-TiO₂ samples of 1 wt% and 5 wt% were prepared by physical mixing, and their optical and structural properties were analyzed by

UV-Vis spectrophotometry and X-ray diffraction (XRD). The VOC removal performance of pure TiO₂, 1 wt% AgNP-TiO₂, and 5 wt% AgNP-TiO₂ was then compared under UV light and fluorescent (visible) light using paint-coated plastic containers as a model indoor surface.

METHODS AND MATERIALS

Materials

A commercial TiO₂ spray (Pure8, 10 wt% TiO₂, 90 mL bottle, Pure8, USA) was used as the TiO₂ source. Colloidal silver solution (30 nm AgNP, 30 ppm, NutriNoche, USA), sold as an antimicrobial supplement, was used as the AgNP source. Quick-drying floor paint (Rustins Quick Dry Floor Paint, 1 L, Rustins Ltd., UK) was used as a VOC-emitting material to simulate an indoor surface that releases VOC after application. Distilled water was used for the dilution of samples in UV-Vis spectrophotometry. All materials were used as received without further purification.

Preparation of AgNP-TiO₂ Samples by Physical Mixing

Two AgNP-TiO₂ samples were prepared with different AgNP loadings, denoted as 1 wt% AgNP-TiO₂ and 5 wt% AgNP-TiO₂. For the 1 wt% AgNP-TiO₂ sample, 30.67 mL of 30 ppm AgNP solution was added to 1.0 g of TiO₂ spray solution. For the 5 wt% AgNP-TiO₂ sample, 76.68 mL of 30 ppm AgNP solution was added to 0.5 g of TiO₂ spray solution. The labels "1 wt%" and "5 wt%" are used as nominal sample names throughout this paper. Based on the amount of AgNP and TiO₂ used in the preparation, the actual Ag to TiO₂ mass ratios are approximately 0.92 wt% for the 1 wt% sample and 4.6 wt% for the 5 wt% sample. The 5 wt% sample contains about five times more AgNP per unit mass of TiO₂ than the 1 wt% sample, and this difference in AgNP loading is the basis for comparing the two samples. Each mixture was prepared by manual mixing in a glass bottle, followed by inversion for around one minute to obtain a homogeneous suspension. No heating, sonication, or additional chemical treatment was applied. The mixed solution was then transferred to a spray bottle for the surface coating step. Pure TiO₂ spray, taken directly from the Pure8 bottle without any modification, was used as the control sample.

Characterization

The optical and structural properties of pure TiO₂, 1 wt% AgNP-TiO₂, and 5 wt% AgNP-TiO₂ were analyzed

by UV-Vis spectrophotometry and X-ray diffraction (XRD). UV-Vis absorption spectra were recorded using a Lambda 265 spectrophotometer (PerkinElmer, USA) over the wavelength range of 250 to 800 nm with 32 scans. Because the absorbance value of the original samples was above 3, which is outside the linear response range of the instrument, all samples were diluted with distilled water at a ratio of 1:100 (sample:water) before measurement. Distilled water was used as the reference.

XRD analysis was carried out using an Empyrean diffractometer (Malvern Panalytical, UK) with CuK α radiation ($\lambda = 1.5406 \text{ \AA}$) operated at 40 kV and 30 mA. The diffraction patterns were collected over a 2θ range of 20° to 80° with a step size of 0.01°. The crystal phases of TiO₂ and the presence of AgNP were identified using X'Pert HighScore Plus software with the PDF-4 powder diffraction file database.

VOC Removal Test

The VOC removal performance was tested under two lighting conditions. The first condition used a UV LED flashlight (365 nm, 15 W, LET'S RESIN, USA), and the second condition used a fluorescent lamp (F32T8, 32 W, 48 inch, 6500K daylight, Konideke, USA). All experiments were done at 25 °C and 65% relative humidity. These conditions are similar to common indoor environments.

A stackable polypropylene container of 6.5 quart (about 6.1 L, IRIS USA, USA) was used as a model indoor space for each experiment. First, the interior wall of the container was coated with 5 mL of Rustins quick-dry floor paint by a brush. The container was then left to dry for 24 hours at room temperature. After this drying step, 5 mL of one of the three spray samples (pure TiO₂, 1 wt% AgNP-TiO₂, or 5 wt% AgNP-TiO₂) was sprayed on the painted surface as evenly as possible. The container was left to dry again for another 24 hours. This second drying step was done to make sure that the coating was attached to the surface well.

After both drying steps were finished, a portable 10-in-1 air quality monitor (TVOC range 0.000 to 9.999 mg/m³, accuracy 0.001 mg/m³) was put inside the container. The container was then covered with plastic wrap so that VOC could not leak out. Before the light was turned on, the container was kept in a dark environment so that the VOC released from the paint could accumulate inside the container. The TVOC concentration was monitored during this dark step, and the step was considered complete when the TVOC reading reached around 0.5 mg/m³ and the variation stayed below the minimum

measurement unit of the monitor (0.001 mg/m³) for 5 minutes. This criterion was used to make sure that the starting TVOC concentration was reproducible across all trials. Once this condition was met, the dark step was ended and the light exposure was started. In the UV condition, the UV LED flashlight was put about 10 cm above the container. In the fluorescent condition, the fluorescent tube was put about 30 cm above the container. The TVOC concentration was read every 15 minutes for 3 hours.

For each sample, the test under each lighting condition was done four times (N = 4). An equal-variance independent two-sample t-test (Student's t-test) was used to check if there was a difference between the 1 wt% AgNP-TiO₂ and 5 wt% AgNP-TiO₂ results. The t-test was done in Microsoft Excel at a 5% significance level.

RESULTS AND DISCUSSION

UV-Vis Spectroscopy

The UV-Vis absorption spectra of pure TiO₂, 1 wt% AgNP-TiO₂, and 5 wt% AgNP-TiO₂ are presented (Figure 1). All three samples gave strong absorption below 380 nm. This absorption is the band gap absorption of anatase TiO₂, which corresponds to about 3.2 eV. The absorption edge of pure TiO₂ was located at about 380 nm. Above 400 nm, pure TiO₂ showed almost no absorption. This is in line with the optical property of anatase TiO₂ known from the literature (14).

In the spectra of 1 wt% AgNP-TiO₂ and 5 wt% AgNP-TiO₂, a new peak was found at around 430 nm (Figure 1). The peak did not appear in pure TiO₂. The position of this peak is in the range usually reported for the surface plasmon resonance (SPR) band of spherical AgNP around 30 nm in size (15). The exact SPR position can shift between 400 and 450 nm depending on the surrounding medium. So the 430 nm peak indicates that the AgNP kept its plasmonic property after being mixed with the TiO₂ spray.

The intensity of the SPR peak was higher in 5 wt% AgNP-TiO₂ than in 1 wt% AgNP-TiO₂. This trend follows the AgNP loading. More AgNP in the same volume gives more plasmonic centers, so the SPR signal becomes stronger. The peak intensity in this study, however, was lower than the intensity reported in some previous studies on 1 to 3 wt% AgNP-TiO₂ prepared by wet chemical synthesis. Two reasons can be proposed.

The first reason is sample dilution. The original samples had an absorbance higher than 3 at the band

gap region. An absorbance above 3 is outside the linear range of the spectrophotometer (16). So all three samples were diluted with distilled water at a ratio of 1:100 before measurement. After dilution, the AgNP concentration in the cuvette dropped to a sub-ppm level. The SPR signal naturally became weaker because of this dilution. The second reason is the capping agent on the AgNP. The AgNP in this study was obtained from a commercial colloidal silver product. Commercial colloidal silver is usually stabilized by capping agents such as citrate or other surface ligands (17). The capping agents keep the particles dispersed in water and prevent aggregation. At the same time, the capping agent layer screens the electric field at the AgNP surface. This screening dampens the collective oscillation of the surface conduction electrons. The SPR intensity becomes lower as a result. AgNP made by wet chemical synthesis can have thinner or less complete capping, which often gives stronger SPR signals at the same AgNP loading.

The 200 to 380 nm region also showed an increase in absorbance as the AgNP loading increased. This was not expected from the band gap absorption of TiO₂ alone. The TiO₂ amount in the three samples was similar. So another contribution to the UV absorbance must come from the AgNP itself. One contribution is the absorption

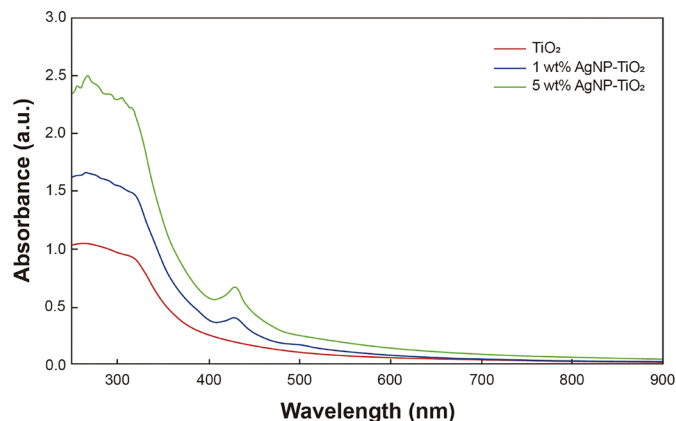


Figure 1. UV-Vis absorption spectra of pure TiO₂, 1 wt% AgNP-TiO₂, and 5 wt% AgNP-TiO₂ measured over the wavelength range of 250 to 900 nm. All samples were diluted with distilled water at a 1:100 ratio before measurement using a Lambda 265 spectrophotometer (PerkinElmer, USA) with 32 scans. The absorption edge around 380 nm corresponds to the band gap absorption of anatase TiO₂. The peak at around 430 nm in the AgNP-TiO₂ samples corresponds to the surface plasmon resonance band of AgNP and increases in intensity with the AgNP loading.

tail of AgNP, which extends from the SPR peak toward shorter wavelengths. Another contribution is Rayleigh scattering by AgNP. Rayleigh scattering is stronger at shorter wavelengths and would raise the apparent absorbance in the UV region. Beyond 500 nm, only the 5 wt% sample showed a slight baseline above zero. This long-wavelength baseline is also likely due to scattering from a higher amount of AgNP in the 5 wt% sample.

The UV-Vis result confirms that physical mixing of commercial colloidal silver and TiO₂ spray produces a sample with a clear SPR peak in the visible region. This is the first piece of evidence that the mixed sample can act as a visible-light driven photocatalyst.

XRD Analysis

The XRD patterns of pure TiO₂, 1 wt% AgNP-TiO₂, and 5 wt% AgNP-TiO₂ are presented (Figure 2). All three samples showed the same set of diffraction peaks. The peaks were assigned to the anatase and rutile phases of TiO₂ by comparison with the PDF-4 database. The peaks marked “A” correspond to anatase. The peaks marked “R” correspond to rutile. In all three samples, the anatase peaks were much stronger than the rutile peaks. The TiO₂ used in this study is therefore mainly in the anatase phase, with only a small amount of rutile.

The dominance of anatase is a favorable feature for photocatalytic application. Anatase generally shows higher photocatalytic activity than rutile. Rutile is the

more thermodynamically stable phase. The reason commonly given in the literature is that anatase has a longer charge carrier lifetime (18). A longer lifetime means more electrons and holes reach the surface and react with adsorbed species before recombination.

The peak positions of anatase and rutile did not shift after AgNP was added (Figure 2). This is an important observation. A peak shift would be expected if AgNP had formed Ag-O-Ti chemical bonds at the TiO₂ surface. A peak shift would also be expected if Ag atoms had substituted Ti atoms in the TiO₂ lattice. Both situations cause lattice distortion, and lattice distortion changes the diffraction angle. No peak shift was observed in this study. So the TiO₂ crystal structure was preserved during physical mixing. AgNP exists as a separate phase in the sample, not built into the TiO₂ lattice.

The peaks of AgNP itself were difficult to identify in the XRD patterns of both 1 wt% and 5 wt% AgNP-TiO₂ (Figure 2). Three reasons can be proposed. The first reason is the low AgNP loading. The detection limit of XRD is typically around 2 to 5 wt%. The exact limit depends on the crystallinity contrast between the analyte and the matrix. Even 5 wt% is close to this limit, and 1 wt% is below it. The second reason is the small particle size. The AgNP in this study had a size of about 30 nm. A particle of 30 nm contains around 10⁵ atoms (19). This number of atoms is small for producing sharp diffraction peaks. The Scherrer effect also broadens the AgNP peaks at this particle size. A broadened peak merges into the baseline more easily (19). The third reason is the requirement of long-range periodicity. XRD relies on long-range crystalline order to give clear peaks. The AgNP in this study was dispersed in a thin coating that dried from a water-based mixture. The AgNP particles in the dried coating are individually crystalline, but they are not connected into continuous crystalline domains. Without large continuous domains, the diffraction signal stays weak even when the AgNP itself is crystalline.

The UV-Vis and XRD results together indicate that AgNP and TiO₂ coexist in the mixed sample as physically separate species. The AgNP retains its plasmonic character, as seen from the SPR peak in UV-Vis. The TiO₂ retains its anatase-dominant crystal structure, as seen from the unchanged peak positions in XRD. Neither spectrum shows any sign of chemical bonding between AgNP and TiO₂.

VOC Removal under UV Light

The TVOC concentration was monitored over 3 hours under UV LED illumination at 365 nm for pure TiO₂,

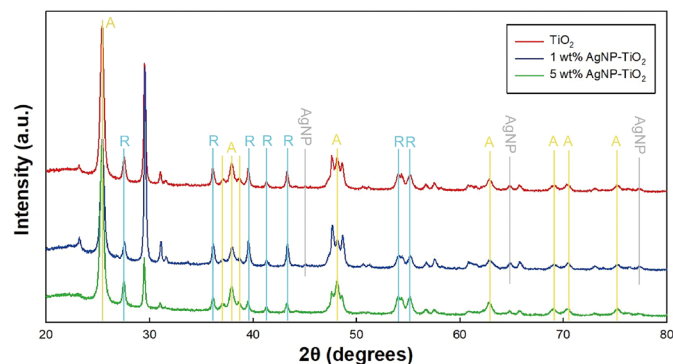


Figure 2. XRD patterns of pure TiO₂ (red), 1 wt% AgNP-TiO₂ (blue), and 5 wt% AgNP-TiO₂ (green) collected over a 2θ range of 20° to 80° using an Empyrean diffractometer (Malvern Panalytical, UK) with CuKα radiation (λ = 1.5406 Å) at 40 kV and 30 mA. Peaks marked “A” (yellow lines) correspond to the anatase phase of TiO₂, and peaks marked “R” (turquoise lines) correspond to the rutile phase. Peaks marked “AgNP” (gray lines) indicate the expected positions of metallic silver. The patterns are vertically offset for clarity.

1 wt% AgNP-TiO₂, and 5 wt% AgNP-TiO₂ (Figure 3). Each curve represents the mean of four independent measurements ($N = 4$), and the error bars correspond to the standard deviation. All three samples reduced the TVOC concentration over time, which confirms that TiO₂-based photocatalysis operates under UV light as expected. After 3 hours of UV exposure, 5 wt% AgNP-TiO₂ achieved the largest reduction in TVOC, followed by 1 wt% AgNP-TiO₂, and pure TiO₂ showed the smallest reduction (Figure 3). The difference between pure TiO₂ and 1 wt% AgNP-TiO₂ was clear throughout the experiment. The difference between 1 wt% and 5 wt% AgNP-TiO₂ was smaller but still visible in most time intervals.

An equal-variance two-sample t-test was performed between 1 wt% and 5 wt% AgNP-TiO₂ at each 15-minute interval to evaluate the statistical significance of the difference. From 15 to 45 minutes, the p-values were below 0.01 (specifically 0.0076 at 15 minutes, 0.0033 at 30 minutes, and 0.0062 at 45 minutes). The two samples were already different in the early stage of the reaction. At 60 minutes, the p-value rose to 0.25, which is well above the 5% significance level. The difference between 1 wt% and 5 wt% became statistically insignificant at this single time point. From 75 minutes onward, the

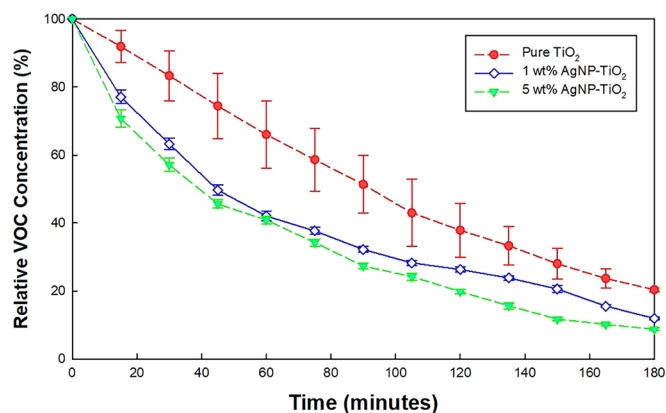


Figure 3. Relative VOC concentration (%) over 3 hours under UV LED illumination (365 nm, 15 W) for pure TiO₂ (red), 1 wt% AgNP-TiO₂ (blue), and 5 wt% AgNP-TiO₂ (green) sprayed onto paint-coated polypropylene containers. The initial TVOC concentration was stabilized at around 0.5 mg/m³ in a dark environment before light exposure. The TVOC concentration was recorded at 15-minute intervals using a 10-in-1 portable air quality monitor. Each data point represents the mean of four independent measurements ($N = 4$), and the error bars correspond to one standard deviation.

p-values dropped back below 0.01 (0.0035 at 75 minutes and 0.00019 at 90 minutes) and continued to decrease (1.1×10^{-5} at 120 minutes, 6.8×10^{-6} at 135 minutes, and 2.7×10^{-6} at 150 minutes).

The 60-minute paradox can be interpreted from a kinetic point of view. One possible interpretation is that both samples reached a temporary saturation around 60 minutes. By that time, most of the VOC molecules accessible on the coated surface had already been decomposed by the photocatalytic reaction (20). At this saturation point, the rate-limiting step shifts from the intrinsic photocatalytic activity to the supply of fresh VOC from the underlying paint. Both samples become limited by the same diffusion-controlled process, so the gap between them temporarily narrows.

After 60 minutes, the VOC release from the paint continued and the reaction settled into a slower steady state. The difference between 1 wt% and 5 wt% AgNP-TiO₂ reappeared during this stage. The 1 wt% sample reached its plateau performance earlier because it has fewer plasmonic centers for the same TiO₂ amount. The 5 wt% sample continued to remove VOC at a higher rate, since the additional AgNP provided more SPR-mediated absorption sites that contribute extra charge carriers to the TiO₂. The very small p-values from 135 minutes onward (around 10^{-5} to 10^{-6}) support this interpretation. The gap between the two samples kept widening during the steady-state stage.

The standard deviation of pure TiO₂ was larger than that of the AgNP-TiO₂ samples at most time points (Figure 3). This is likely because pure TiO₂ depends only on direct UV absorption for activation, and small fluctuations in lamp position, ambient light, or sample placement translate into larger fluctuations in the photocatalytic rate. The AgNP-TiO₂ samples have an additional plasmonic absorption channel that broadens the spectral range of activation. This additional channel makes the AgNP-TiO₂ samples less sensitive to small variations in the UV intensity.

The UV experiment shows that adding AgNP to TiO₂ by physical mixing improves photocatalytic VOC removal even under UV illumination, where pure TiO₂ is already active. The improvement is statistically significant for almost the entire 3-hour duration, except for the brief saturation point at 60 minutes. This indicates that the SPR effect of AgNP contributes not only in the visible region but also under UV illumination, likely through hot electron injection from AgNP into the conduction band of TiO₂, which provides an additional source of charge carriers.

VOC Removal under Visible (Fluorescent) Light

The TVOC concentration was monitored over 3 hours under fluorescent lamp illumination at 6500 K daylight color temperature for pure TiO₂, 1 wt% AgNP-TiO₂, and 5 wt% AgNP-TiO₂ (Figure 4). Each curve represents the mean of four independent measurements ($N = 4$), and the error bars correspond to the standard deviation. All three samples reduced the TVOC concentration over time, which indicates that VOC removal occurred even under indoor-type lighting conditions.

After 3 hours of fluorescent exposure, the remaining TVOC was about 3.84% of the initial value for 5 wt% AgNP-TiO₂, 8.60% for 1 wt% AgNP-TiO₂, and 13.67% for pure TiO₂ (Figure 4). The performance order, 5 wt% > 1 wt% > pure TiO₂, was the same as in the UV experiment. The gap between pure TiO₂ and the AgNP-TiO₂ samples was larger under fluorescent light than under UV light. The gap between 1 wt% and 5 wt% AgNP-TiO₂ was also more consistent across the 3-hour duration. An equal-variance two-sample t-test was performed for three pairwise comparisons at each 15-minute interval. The p-values for pure TiO₂ versus 1 wt% AgNP-TiO₂ were below 0.01 throughout the experiment, ranging from 3.0×10^{-3} at 15 minutes to 1.1×10^{-3} at 180 minutes, with the smallest p-value of 2.9×10^{-6} at

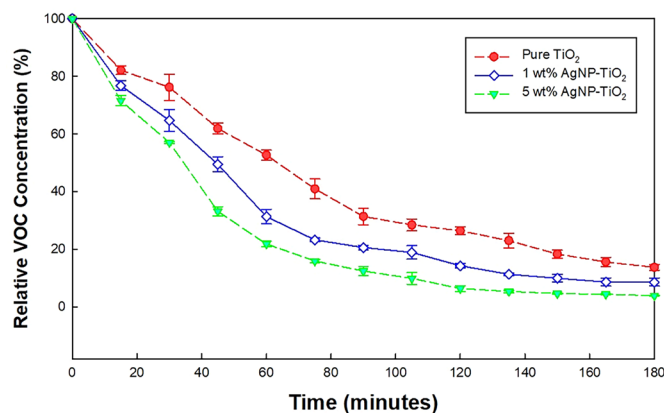


Figure 4. Relative VOC concentration (%) over 3 hours under fluorescent lamp illumination (32 W) for pure TiO₂ (red), 1 wt% AgNP-TiO₂ (blue), and 5 wt% AgNP-TiO₂ (green) sprayed onto paint-coated polypropylene containers. The initial TVOC concentration was stabilized at around 0.5 mg/m³ in a dark environment before light exposure. The TVOC concentration was recorded at 15-minute intervals using a 10-in-1 portable air quality monitor. Each data point represents the mean of four independent measurements ($N = 4$), and the error bars correspond to one standard deviation.

120 minutes. The p-values for pure TiO₂ versus 5 wt% AgNP-TiO₂ were even smaller, falling between 1.0×10^{-4} and 1.1×10^{-6} in most intervals and reaching 6.7×10^{-8} at 60 minutes. The p-values for 1 wt% versus 5 wt% AgNP-TiO₂ were also below 0.01 at every time point, ranging from 4.7×10^{-3} at 15 minutes to 5.8×10^{-4} at 180 minutes. The 60-minute paradox observed in the UV experiment did not appear under fluorescent light. All three pairwise comparisons remained statistically significant from 15 to 180 minutes without any exception.

The larger gap between pure TiO₂ and AgNP-TiO₂ under fluorescent light follows directly from the spectral mismatch between TiO₂ and the light source. A fluorescent lamp emits mainly in the visible region, with only a small UV component. Pure TiO₂ has a band gap of about 3.2 eV, which corresponds to the UV region. So pure TiO₂ can only use the small UV fraction of fluorescent light to generate electron-hole pairs. Its photocatalytic activity is limited by this small UV fraction. AgNP-TiO₂ samples, in contrast, can also use the visible fraction through SPR absorption by the AgNP. The energy absorbed by AgNP is transferred to TiO₂ through near-field electromagnetic coupling or hot electron injection, which gives TiO₂ a second source of charge carriers that pure TiO₂ does not have (21).

The absence of the 60-minute paradox under fluorescent light is also consistent with this interpretation. Under UV illumination, both pure TiO₂ and AgNP-TiO₂ are activated by the same direct band gap absorption mechanism. The temporary saturation at 60 minutes affects all samples in a similar way, so the gap between 1 wt% and 5 wt% briefly narrows. Under fluorescent light, pure TiO₂ is much less active overall, and the rate-limiting step for pure TiO₂ is the small UV fraction rather than VOC supply. The AgNP-TiO₂ samples maintain a higher and steadier rate throughout the experiment because their plasmonic absorption channel provides a continuous additional source of charge carriers. The two AgNP-TiO₂ samples also stayed clearly separated at every time point because the visible-light absorption scales directly with the AgNP loading, and 5 wt% has more SPR centers than 1 wt%. The fluorescent light experiment confirms that AgNP-TiO₂ made by simple physical mixing functions as a visible-light driven photocatalyst, with much higher VOC removal than pure TiO₂ under indoor lighting conditions.

Chemistry Discussion and Limitations

The main observation from this study is that physical mixing of two commercial products produced a working

visible-light photocatalyst without any chemical synthesis step. The UV-Vis spectra showed a clear SPR peak from AgNP, and the XRD patterns showed no peak shift after AgNP was added. AgNP and TiO₂ therefore coexist in the sample as physically separate species, not chemically bonded together. Despite the absence of chemical bonding, the AgNP-TiO₂ samples removed VOC much more effectively than pure TiO₂ under fluorescent light.

This result is consistent with the photon-driven nature of the SPR effect. SPR is an optical phenomenon. When AgNP absorbs visible photons, the conduction electrons on the AgNP surface oscillate collectively at the resonance frequency (22). This collective oscillation builds a strong near-field electromagnetic enhancement around the AgNP. If a TiO₂ particle is located close to this near-field, the enhanced electromagnetic field can drive electron-hole pair generation in the TiO₂ even at photon energies below the TiO₂ band gap (23). Hot electron injection from AgNP into the conduction band of TiO₂ is another possible pathway, in which energetic electrons generated by SPR decay are transferred across the AgNP-TiO₂ interface (24). Both mechanisms operate through space rather than through a chemical bond. Ag-O-Ti junction formation is therefore not required, and physical proximity between AgNP and TiO₂ in the dried coating appears to be sufficient for plasmonic sensitization to occur.

This is the chemistry insight from this study. Most previous reports on AgNP-TiO₂ used wet chemical synthesis, sol-gel, or photodeposition methods (13, 14). These methods were designed to establish direct contact between AgNP and TiO₂ at the atomic level. The present results show that for plasmonic sensitization to occur, atomic-level contact may not be necessary. As long as the two species end up close to each other in the dried coating, the SPR effect can still couple to TiO₂. This finding suggests a simpler route to plasmonic photocatalyst coatings that does not require synthetic equipment or trained handling.

Several limitations should be mentioned. The SPR peak intensity in the UV-Vis spectra was lower than the intensity reported in previous studies that used wet chemical synthesis. This is partly due to the 1:100 dilution required for the measurement, but the capping agents on the commercial AgNP also likely contributed (17). A direct comparison of the photocatalytic rate per AgNP between the physically mixed sample and a wet-chemistry sample at the same AgNP loading was not performed in this study. So it cannot yet be concluded whether physical mixing is as efficient as chemical

synthesis on a per-particle basis, only that it is sufficient to give clear visible-light activity.

The labels “1 wt%” and “5 wt%” in this study are nominal sample names. Based on the preparation amounts and the 10 wt% TiO₂ content of the spray, the actual Ag-to-TiO₂ mass ratios are approximately 0.92 wt% and 4.6 wt%, as described in Section 2.2. The comparison between the two samples should therefore be understood as a comparison between a lower and a higher AgNP loading, where the higher loading is about five times the lower one. In addition, these ratios are based on the amounts used during the mixing, and the actual amount of AgNP retained on the surface after drying was not separately quantified by elemental analysis such as Inductively Coupled Plasma Optical Emission Spectroscopy (ICP-OES) or Energy Dispersive X-ray Spectroscopy (EDS). Some of the AgNP particles may be leached during the spraying and drying steps, and thus the real Ag loading on the tested surface could be different from the labeled value. A direct quantification of the deposited Ag would make the relationship between AgNP loading and photocatalytic performance more accurate.

Hence, the two materials used in this study were commercial products, which are a colloidal silver solution and a TiO₂ spray. Commercial formulations can vary between production batches in particle size, particle concentration, capping agent content, and additives, and these factors are not fully disclosed by the manufacturers. Such batch-to-batch variability could affect the SPR intensity and the photocatalytic performance, and it may reduce the reproducibility when the same products are purchased at a different time or from a different supplier. This is an inherent limitation of using commercial products instead of materials synthesized under controlled laboratory conditions, although the use of commercial products is also the main practical advantage of this approach.

Besides the limitations of the commercial materials, the VOC source in the experiments was a single type of paint, which emits a mixture of VOCs. The concentration was measured with a portable TVOC monitor, which reports only the total VOC value as a sum signal and cannot distinguish which individual VOC species are being degraded. Because of this, the total VOC concentration was confirmed to decrease, but the selectivity of the photocatalysis for specific VOC species, such as formaldehyde, benzene, or toluene, could not be determined. A compound-specific analytical method such as gas chromatography-mass spectrometry (GC-

MS) would be needed to identify which VOC species are removed and at what rate, and this is left for future work. In addition, other VOC sources such as adhesives or new furniture emit different VOC profiles, so the removal behavior observed here may not directly apply to those sources (25).

The fluorescent lamp used in this study emits at 6500 K daylight color temperature, which includes a small UV-A component (26). This means that under the “fluorescent” condition, pure TiO₂ can also be slightly activated by the residual UV part of the spectrum. This partly explains why pure TiO₂ still showed some VOC removal under fluorescent light. A pure visible-light source without any UV component would give a cleaner test of the SPR effect, and this can be a direction for follow-up work.

The test was conducted inside a 6.1 L stackable container, which is much smaller than a real room. Scale-up effects, such as longer light path lengths or non-uniform light intensity on a real wall, were not examined. Whether the simple physical mixing method holds up at the scale of an entire room remains a separate question that requires further investigation.

CONCLUSION

This study tested whether a simple physical mixing of two commercial products, a colloidal silver solution and a TiO₂ spray, can give a visible-light driven photocatalyst for indoor VOC removal. The UV-Vis spectra of both 1 wt% and 5 wt% AgNP-TiO₂ showed a clear SPR peak at around 430 nm. The XRD patterns showed no peak shift after AgNP was added. These two results together indicate that AgNP and TiO₂ stay as separate species in the mixed sample. The VOC removal experiment under fluorescent light gave a clear performance order. After 3 hours, the remaining TVOC was 3.84% for 5 wt% AgNP-TiO₂, 8.60% for 1 wt% AgNP-TiO₂, and 13.67% for pure TiO₂. The chemistry insight from these results is that plasmonic sensitization of TiO₂ does not need chemical bonding between AgNP and TiO₂. The SPR effect works through space. The near-field electromagnetic enhancement and hot electron injection are both optical processes that do not require a chemical bond. Physical proximity in the dried coating is enough. The limitations of this study include the weaker SPR peak intensity from dilution and capping agents, the lack of selectivity information for individual VOC species, and the small container scale of 6.1 L. Future work should compare physically mixed samples and wet-chemistry

samples at the same AgNP loading. Future work should also test individual VOC species such as formaldehyde or benzene and check the scale-up behavior in a room-sized environment. Physical mixing of commercial products offers an accessible way to make visible-light photocatalyst coatings for indoor air treatment.

CONFLICT OF INTEREST

The authors declare that there are no conflicts of interest related to this work.

REFERENCES

1. Klepeis NE, *et al.* The National Human Activity Pattern Survey (NHAPS): a resource for assessing exposure to environmental pollutants. *J Expo Anal Environ Epidemiol.* 2001; 11 (3): 231-252. <https://doi.org/10.1038/sj.jea.7500165>
2. Joshi SM. The sick building syndrome. *Indian J Occup Environ Med.* 2008; 12 (2): 61-64. <https://doi.org/10.4103/0019-5278.43262>
3. Redlich CA, *et al.* Sick-building syndrome. *Lancet.* 1997; 349 (9057): 1013-1016. [https://doi.org/10.1016/S0140-6736\(96\)07220-0](https://doi.org/10.1016/S0140-6736(96)07220-0)
4. World Health Organization, Regional Office for Europe. Indoor air pollutants: exposure and health effects: report on a WHO meeting, Nördlingen, 8-11 June 1982. ICP/RCE 304 (2). Copenhagen: WHO Regional Office for Europe; 1983.
5. Vardoulakis S, *et al.* Indoor exposure to selected air pollutants in the home environment: a systematic review. *Int J Environ Res Public Health.* 2020; 17 (23): 8972. <https://doi.org/10.3390/ijerph17238972>
6. Du Z, *et al.* Risk assessment of population inhalation exposure to volatile organic compounds and carbonyls in urban China. *Environ Int.* 2014; 73: 33-45. <https://doi.org/10.1016/j.envint.2014.06.014>
7. Huang KC, *et al.* Degradation of volatile organic compounds with thermally activated persulfate oxidation. *Chemosphere.* 2005; 61 (4): 551-560. <https://doi.org/10.1016/j.chemosphere.2005.02.032>
8. Zhang Y, *et al.* Photocatalytic oxidation for volatile organic compounds elimination: from fundamental research to practical applications. *Environ Sci Technol.* 2022; 56 (23): 16582-16601. <https://doi.org/10.1021/acs.est.2c05444>
9. Schneider J, *et al.* Understanding TiO₂ photocatalysis: mechanisms and materials. *Chem Rev.* 2014; 114 (19): 9919-9986. <https://doi.org/10.1021/cr5001892>
10. Nakata K, *et al.* TiO₂ photocatalysis: design and applications. *J Photochem Photobiol C.* 2012; 13

- (3): 169-189. <https://doi.org/10.1016/j.jphotochemrev.2012.06.001>
11. Pelaez M, *et al.* A review on the visible light active titanium dioxide photocatalysts for environmental applications. *Appl Catal B*. 2012; 125: 331-349. <https://doi.org/10.1016/j.apcatb.2012.05.036>
 12. Hagfeldt A, *et al.* Dye-sensitized solar cells. *Chem Rev*. 2010; 110 (11): 6595-6663. <https://doi.org/10.1021/cr900356p>
 13. Linic S, *et al.* Plasmonic-metal nanostructures for efficient conversion of solar to chemical energy. *Nat Mater*. 2011; 10 (12): 911-921. <https://doi.org/10.1038/nmat3151>
 14. Murphy AB. Band-gap determination from diffuse reflectance measurements of semiconductor films, and application to photoelectrochemical water-splitting. *Sol Energy Mater Sol Cells*. 2007; 91 (14): 1326-1337. <https://doi.org/10.1016/j.solmat.2007.05.005>
 15. Mock JJ, *et al.* Shape effects in plasmon resonance of individual colloidal silver nanoparticles. *J Chem Phys*. 2002; 116 (15): 6755-6759. <https://doi.org/10.1063/1.1462610>
 16. Owen T. Fundamentals of UV-visible spectroscopy: a primer. Waldbronn: Agilent Technologies; 1996.
 17. Pinto VV, *et al.* Long time effect on the stability of silver nanoparticles in aqueous medium: effect of the synthesis and storage conditions. *Colloids Surf A Physicochem Eng Asp*. 2010; 364 (1-3): 19-25. <https://doi.org/10.1016/j.colsurfa.2010.04.015>
 18. Luttrell T, *et al.* Why is anatase a better photocatalyst than rutile? Model studies on epitaxial TiO₂ films. *Sci Rep*. 2014; 4: 4043. <https://doi.org/10.1038/srep04043>
 19. Cullity BD, Stock SR. Elements of X-ray diffraction. Upper Saddle River: Prentice Hall; 2001.
 20. Mo J, *et al.* Photocatalytic purification of volatile organic compounds in indoor air: a literature review. *Atmos Environ*. 2009; 43 (14): 2229-2246. <https://doi.org/10.1016/j.atmosenv.2009.01.034>
 21. Awazu K, *et al.* A plasmonic photocatalyst consisting of silver nanoparticles embedded in titanium dioxide. *J Am Chem Soc*. 2008; 130 (5): 1676-1680. <https://doi.org/10.1021/ja076503n>
 22. Kelly KL, *et al.* The optical properties of metal nanoparticles: the influence of size, shape, and dielectric environment. *J Phys Chem B*. 2003; 107 (3): 668-677. <https://doi.org/10.1021/jp026731y>
 23. Linic S, *et al.* Photochemical transformations on plasmonic metal nanoparticles. *Nat Mater*. 2015; 14 (6): 567-576. <https://doi.org/10.1038/nmat4281>
 24. Clavero C. Plasmon-induced hot-electron generation at nanoparticle/metal-oxide interfaces for photovoltaic and photocatalytic devices. *Nat Photonics*. 2014; 8 (2): 95-103. <https://doi.org/10.1038/nphoton.2013.238>
 25. Wang S, *et al.* Volatile organic compounds in indoor environment and photocatalytic oxidation: state of the art. *Environ Int*. 2007; 33 (5): 694-705. <https://doi.org/10.1016/j.envint.2007.02.011>
 26. Sayre RM, *et al.* Dermatological risk of indoor ultraviolet exposure from contemporary lighting sources. *Photochem Photobiol*. 2004; 80 (1): 47-51. <https://doi.org/10.1562/2004-02-03-RA-074.1>, <https://doi.org/10.1111/j.1751-1097.2004.tb00048.x>